Title

Microbial Cleavage of C–F Bonds in Two C6 Per- and Polyfluorinated Compounds via Reductive Defluorination

Journal

Environmental Science and Technology, 54(22)

ISSN

0013-936X

Authors

Yu, Yaochun
Zhang, Kunyang
Li, Zhong
et al.

Publication Date

2020-11-17

DOI

10.1021/acs.est.0c04483

Environmental Science & Technology

pubs.acs.org/est

Article

Microbial Cleavage of C−F Bonds in Two C_6 Per- and Polyfluorinated Compounds via Reductive Defluorination

Yaochun Yu, Kunyang Zhang, Zhong Li, Changxu Ren, Jin Chen, Ying-Hsuan Lin, Jinyong Liu, and Yujie Men*

Cite This: *Environ. Sci. Technol.* 2020, 54, 14393−14402

Read Online

ACCESS | Metrics & More | Article Recommendations | Supporting Information

ABSTRACT: The C−F bond is one of the strongest single bonds in nature. Although microbial reductive dehalogenation is well known for the other organohalides, no microbial reductive defluorination has been documented for perfluorinated compounds except for a single, nonreproducible study on trifluoroacetate. Here, we report on C−F bond cleavage in two C_6 per- and polyfluorinated compounds via reductive defluorination by an organohalide-respiring microbial community. The reductive defluorination was demonstrated by the release of F^- and the formation of the corresponding product when lactate was the electron donor, and the fluorinated compound was the sole electron acceptor. The major dechlorinating species in the seed culture, *Dehalococcoides*, were not responsible for the defluorination as no growth of *Dehalococcoides* or active expression of *Dehalococcoides*-reductive dehalogenases was observed. It suggests that minor phylogenetic groups in the community might be responsible for the reductive defluorination. These findings expand our fundamental knowledge of microbial reductive dehalogenation and warrant further studies on the enrichment, identification, and isolation of responsible microorganisms and enzymes. Given the wide use and emerging concerns of fluorinated organics (e.g., per- and polyfluoroalkyl substances), particularly the perfluorinated ones, the discovery of microbial defluorination under common anaerobic conditions may provide valuable insights into the environmental fate and potential bioremediation strategies of these notorious contaminants.

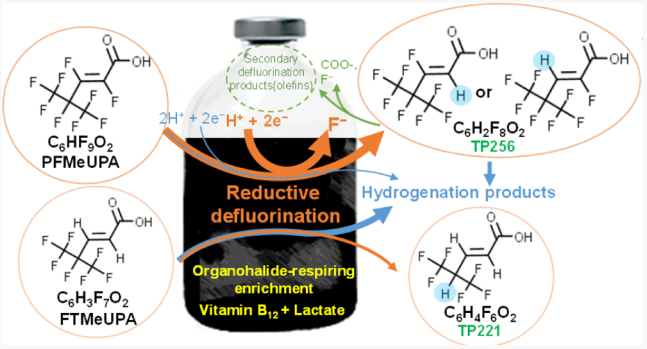

INTRODUCTION

Thousands of organofluorine compounds are on the market, used with diverse applications ranging from surfactants for firefighting and oil production as well as oil/water-repelling materials in commercial goods[1] to refrigerants[2] and reagents in catalysis.[3] Because of their wide applications, the organofluorine compounds, especially the per- and polyfluoroalkyl substances (PFASs), have caused increasing global concerns on their persistence in the environment, bioaccumulation in organisms, and toxicity to human beings and ecosystems.[1] Many of them have been frequently detected in various environments.[4−6] Tremendous efforts have been and are being made to understand the environmental fate and transport of the structurally diverse fluorinated compounds and to develop effective removal strategies. Because of the strong carbon−fluorine (C−F) bond,[7] to date, the defluorination of fluorinated compounds relies on energy-intensive physiochemical approaches.[8−12] Only sporadic studies on microbial defluorination have been reported since the 1960s when the hydrolytic dehalogenase catalyzing aerobic hydrolytic defluorination of monofluoroacetate was identified.[13] Moreover, there has been only one single study showing the stepwise reductive defluorination of trifluoroacetate (TFA, CF_3COOH) to acetate in a methanogenic microbial community,[14] yet it proved to be nonreproducible,[15,16] with no follow-up studies on the responsible microorganisms/enzymes. An isolate from the phylum *Synergistetes* in the absence of known fluoroacetate dehalogenase genes has shown reductive defluorination activities on monofluoroacetate but not TFA when grown on the fermentation of amino acids.[17,18]

For $>C_2$ fluorinated compounds, microbial defluorination has been observed for polyfluorinated telomeric structures (i.e., fluorinated compounds containing CH_2 moieties) under both aerobic and anaerobic conditions,[19−22] yet no microbial defluorination of perfluorinated structures was reported until very recently when Huang and Jaffé observed F^- release from perfluorooctanoic acid (PFOA)/perfluorooctanesulfonic acid

Received: July 8, 2020
Revised: September 6, 2020
Accepted: October 16, 2020
Published: October 29, 2020

(PFOS) in Feammox cultures using Fe^{3+} as the required electron acceptor.[23] However, convincing evidence for microbial reductive defluorination, in terms of F^- release and formation of the reductive defluorination products, is still lacking from all previous studies.

According to the thermodynamic calculation, reductive defluorination of fluorinated compounds is biologically feasible.[24] Thus, one intriguing yet not well-addressed question is that can microbes carry out reductive defluorination of $>C_2$ perfluorinated structures? In this study, we aimed to fill this knowledge gap and investigate microbial reductive defluorination of a variety of per- and polyfluorinated structures. Recent studies reported abiotic reductive defluorination of branched and unsaturated perfluorinated compounds in a vitamin B_{12}−Ti(III) catalytic system at room temperature,[8,25] where Ti(III) recycles and reduces Co(III) in B_{12} into Co(I), the active species carrying out the reductive defluorination.[26] It suggests that reductive defluorination of perfluorinated compounds with similar structures might also be carried out in an anaerobic microbial system, where an enzymatically catalytic system for reductive dehalogenation, such as B_{12}-dependent reductive dehalogenases (RDase), is present.[27−29] We herein used the subcultures of a well-studied dechlorinating enrichment culture and pure dechlorinating cultures to test the biotransformation and biodefluorination of five structurally different per- and polyfluorinated compounds. The biotransformation/biodefluorination products [transformation products (TPs)] were identified, the plausible pathways were further interpreted, and the possible microorganisms involved in the reductive defluorination were discussed. The discovery of microbial defluorination of perfluorinated compounds via the H−F exchange reductive pathway fills the knowledge gap of microbially mediated reductive dehalogenation of organofluorine compounds. The findings shed light on a better understanding of microbial processes that may affect the fate and transport of fluorinated compounds in the environment.

MATERIALS AND METHODS

Chemicals. Standard compounds of perfluoro-*n*-octanoic acid (CAS number: 335-67-1, PFOA), perfluoro-3,7-dimethyloctanoic acid (CAS number: 172155-07-6, PFdiMeOA), (E)-perfluoro(4-methylpent-2-enoic acid) (CAS number: 103229-89-6, PFMeUPA), 4,5,5,5-tetrafluoro-4-(trifluoromethyl)-2-pentenoic acid (CAS number: 243139-64-2, FTMeUPA), and 4,5,5,5-tetrafluoro-4-(trifluoromethyl)pentanoic acid (CAS number: 243139-62-0, FTMePA) were purchased form SynQuest Laboratories (Alachua, FL) and used without further purification. For PFOA, PFdiMeOA, PFMeUPA, FTMeUPA, and FTMePA, 10 mM stock solutions of each standard were prepared anaerobically in autoclaved Milli-Q water in 160 mL sealed serum bottles and stored at room temperature until use. Detailed compound structure information is listed in Table S1.

Cultures and Growth Conditions. The *Dehalococcoides*-containing trichloroethene (TCE)-dechlorinating enrichment (KB1) was generously provided by SiREM Lab (https://www.siremlab.com/). Pure *Dehalococcoides mccartyi* BAV1 (ATCC BAA-2100) and FL2 (ATCC BAA-2098) were purchased from the American Type Culture Collection (ATCC). Pure *Dehalobacter restrictus* was purchased from Deutsche Sammlung von Mikroorganismen und Zellkulturen (DSM-9455). All cultures were maintained in 160 mL sealed serum bottles containing 90 mL of a sterile anaerobic basal medium with 100 μg/L vitamin B_{12} as previously described[30,31] and a 60 mL Ar/CO_2 headspace. Vitamin B_{12} was provided as an essential cofactor for the defluorinating pure cultures. For the maintenance of KB1 culture, 5 mM lactate and 2 μL of neat TCE (ca. 220 μM) were added as the primary electron donor and electron acceptor, respectively, and were readded periodically. The three dechlorinating pure cultures were maintained in the same basal medium with a H_2/Ar/CO_2 headspace. For *D. mccartyi* BAV1, 5 mM acetate and 2 μL of neat *cis*-dichloroethene (DCE) were supplied upon depletion. For *D. mccartyi* FL2 and *D. restrictus*, 5 mM acetate and 2 μL of neat TCE were supplied upon depletion. All cultures were incubated at 34 °C in a dark incubator without shaking.

Biodefluorination Experiments. The dechlorinating enrichment (KB1) (10 mL) or the pure dechlorinating culture was inoculated into 90 mL of the sterile basal medium amended with 5 mM lactate (or acetate for pure cultures) as described above. A sole electron acceptor was added in two scenarios: (1) 75 μM individual organofluorine compound as the defluorination experimental group and (2) 220 μM TCE/*cis*-DCE as the culture activity control. The electron donor (i.e., lactate for KB1 and H_2 for *Dehalococcoides* pure cultures) and the electron acceptors were readded after depletion. The dechlorinating activity was examined by measuring TCE and the dechlorination products via gas chromatography coupled to a mass-selective detector (GC-MSD) (Figure S1). For organofluorine-added cultures, aqueous samples were taken subsequently during the incubation period for the measurement of parent compounds and F^-. Briefly, the culture suspension was centrifuged at 16,000*g* (4 °C for 30 min) for F^- measurement (2 mL) and the liquid chromatography−high-resolution tandem mass spectrometry (LC-HRMS/MS) measurement (2 mL). Cell pellets were stored properly for DNA (−20 °C) and RNA (−80 °C) extraction, respectively. Heat-inactivated biomass controls were set up by inoculating a 10 mL autoclaved (at 121 °C for 20 min for two cycles) culture in the same basal medium amended with the same nutrients including the same concentrations of vitamin B_{12}, the electron donor (lactate for KB1 subcultures and H_2 for *Dehalococcoides* pure cultures), and the electron acceptor (organofluorines). All experimental groups and controls were set up in triplicates.

Fluoride-Ion Measurement by the Ion-Selective Electrode Method. The concentration of the fluoride ion (F^-) in the culture supernatant was determined using an ion-selective electrode (ISE, HACH, Loveland, CO) connected with an HQ30D Portable Multi Meter (HACH). A 100 μg fluoride ionic strength adjustment powder (HACH) was added into 2 mL of the culture supernatant, and the F^- concentration was then measured with the ISE-Multi Meter system. The ISE was calibrated each time before sample measurement according to the manufacturer's instructions. The limit of quantification (LOQ) of ISE was 0.01 mg/L (~0.5 μM) F^-. In addition, ion chromatography (IC) was used to validate the fluoride measurement by ISE. The LOQ of IC was 1 μM F^-. For ISE method validation, six mock samples with F^- concentrations ranging from 0 to 100 μM were prepared in the medium matrix, and three samples were prepared from a real supernatant sample (measured as 32.7 μM by ISE and 31.0 μM by IC) with the addition of 0, 9.5, and 49.8 μM F^- standard. F^- concentrations in all samples were measured by ISE and IC, and the results were compared. The two methods exhibited similar (a 10% or less difference) fluoride concentration measurement results (Figure S2).

https://dx.doi.org/10.1021/acs.est.0c04483
Environ. Sci. Technol. 2020, 54, 14393−14402

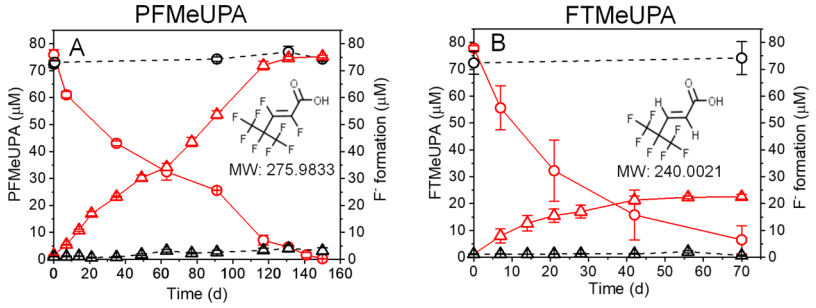

Figure 1. Parent compound removal and fluoride-ion release for PFMeUPA (A) and FTMeUPA (B) (red: biological samples; black: heat-inactivated controls; circles: parent compound; triangles: fluoride ion; error bars indicate the standard deviation of three biological replicates).

Fluoride-Ion Measurement by IC. A Dionex ICS-5000 IC system equipped with a conductivity detector and a Dionex IonPac AS10 Analytical Column (4 × 250 mm) (Thermo Fisher Scientific, Waltham, MA) was used for the ISE validation. The high-purity potassium hydroxide eluent was generated by a Dionex ICS-6000 Eluent Generator with the following gradient: 3 mM for 0−20 min, 40 mM for 20−25 min (slope = 7.4 mM/min), 40 mM for 25−70 min, 3 mM (slope = 7.4 mM/min) for 70−75 min, and 3 mM for 75−95 min. The flow rate was set at 1 mL/min, and the suppressor (AERS_4mm) current was set at 99 mA. Chromeleon 7.1 (Thermo Fisher Scientific) was used for data acquisition and analysis. The retention time of F^- is 17.4 min, which is consistent throughout the analysis (Figure S3).

High-Performance Liquid Chromatography Coupled to High-Resolution Tandem Mass Spectrometry Analysis. Concentrations of the parent compounds and TPs were analyzed by high-performance liquid chromatography (HPLC) coupled to a high-resolution quadrupole orbitrap mass spectrometer (Q Exactive, Thermo Fisher Scientific) in the Metabolomics Lab of Roy J. Carver Biotechnology Center at the University of Illinois at Urbana-Champaign. For HPLC analysis, a 50 μL sample was loaded onto a Zorbax SB-Aq column (a particle size of 5 μm, 4.6 × 50 mm, Agilent) and eluted with 10 mM ammonia formate (A) and methanol (B) at a flow rate of 350 μL/min. The linear gradient for LC separation was 100% A for 0−1 min, 100−2% A for 2−15 min, 2−100% A in 1 min, and 100% A for 16−21 min. For high-resolution mass spectrometry (HRMS), mass spectra were recorded in the full scan mode at a resolution of 70,000 at m/z 200 and a scan range of m/z 50−750 under the negative/positive switch ionization (electrospray ionization) mode. Xcalibur 4.0 and TraceFinder 4.1 EFS (Thermo Fisher Scientific) were used for data acquisition and analysis. The LOQ for each standard compound was determined as the lowest concentration of calibration standards with a detection variation <20%, which is listed in Table S1.

TP Identification. Both suspect screening and nontarget screening were conducted to identify TPs as previously described[32−34] with slight modification. Briefly, the suspect screening was done by TraceFinder 4.1 EFS and Xcalibur 4.0 software (Thermo Fisher Scientific). TP suspect lists were generated by an automated metabolite mass prediction script,[35] which was modified to specifically predict the defluorination products via different biological reaction pathways, including a number of known reduction reactions, hydrolysis reactions, and conjugation reactions at both primary and secondary levels. Plausible TPs were selected based on the following criteria: (i) mass accuracy tolerance < 5 ppm; (ii) isotopic pattern score > 90%; (iii) peak area > 10^8; (iv) increasing trend along time or first increase and then decrease; (v) no formation in heat-inactivated controls and absent in biological samples without any organofluorine addition; and (vi) not detected as an in-source fragment of the parent compound or any other identified TPs (in-source fragments are peaks identified by an MS full scan, which are also MS^2 fragments and have the same retention time and formation pattern as the parent compound or the other TPs). For nontarget screening, the software Sieve 2.2 (Thermo Fisher Scientific) was used for data analysis. The potential TPs were selected based on the same criteria as suspect screening. For TPs with authentic standards (Table S1), MS^2 fragment profiles of both standard compounds and TP candidates were obtained using a data-dependent MS^2 scan based on the exact mass of the precursor ion to elucidate the structures of TPs. MS^2 fragment profiles of TPs without available authentic standards (Table S2) were compared with the predicted fragments by Competitive Fragmentation Modeling for Metabolite Identification (CFM-ID, http://cfmid.wishartlab.com/).[36] The confidence level of structure elucidation for each TP was assigned based on the criteria set up by Schymanski et al.[37] MarvinSketch (version 19.20.0) was used for drawing, displaying, and characterizing chemical structures, ChemAxon (http://www.chemaxon.com).

GC-MSD for TP Analysis in the Gaseous Phase. The headspace in a culture bottle was preconcentrated by solid-phase microextraction (SPME). SPME fibers (silica-fused) coated with polydimethylsiloxane-divinylbenzene (PDMS-DVB, 65 μm) were purchased from Supelco (Bellefonte, PA). The PDMS-DVB-coated SPME fiber has been reported to effectively extract headspace volatile organic compounds such as terpenes, aldehydes, ketones, and alcohols.[38,39] Before sampling, the SPME fiber carried by a needle was conditioned in the gas chromatograph inlet at 260 °C for 15 min[39] During sampling, the SPME needle was injected into the culture bottle and exposed to the headspace for ∼24 h to extract the gas-phase analytes. Analytes retained on the fiber were assessed using GC/electron ionization-mass spectrometry (GC/EI-MS) (Agilent 6890N GC and 5975 MSD, Agilent Technologies, Santa Clara, CA). Headspace samples from PFMeUPA-fed cultures were measured after PFMeUPA was gone. The headspace sample from the heat-inactivated control was also measured, serving as the matrix blank.

The collected SPME samples were manually injected into the gas chromatograph inlet in the splitless mode and desorbed for 3 min at 250 °C. Analytes desorbed from the SPME fiber were separated using a DB-5MS column (a 30 m × 0.25 mm i.d., 0.25 μm film) (Agilent Technologies). The flow rate of the

https://dx.doi.org/10.1021/acs.est.0c04483
Environ. Sci. Technol. 2020, 54, 14393−14402

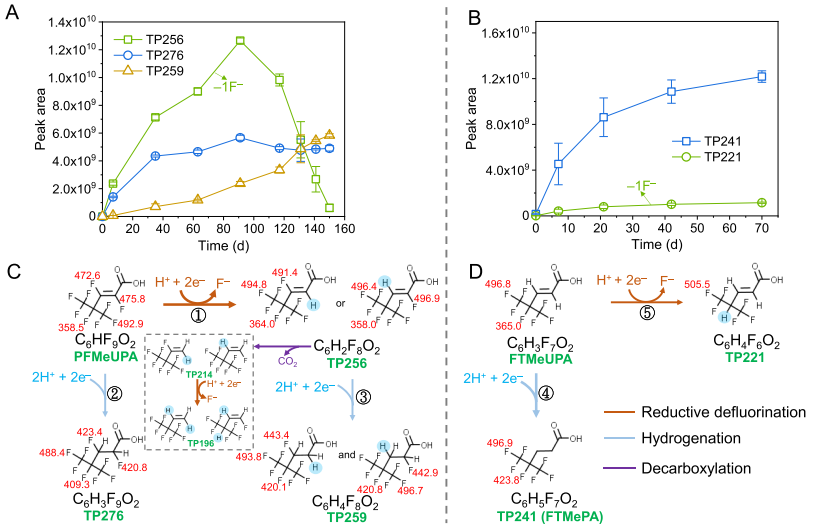

Figure 2. Temporal trend of TPs identified by LC-HRMS/MS during PFMeUPA (A) and FTMeUPA (B) biotransformation (arrows indicate the TPs from reductive defluorination; error bars indicate the standard deviation of three biological replicates); proposed biotransformation pathways of PFMeUPA (C) and FTMeUPA (D) (the red number next to a C−F bond is the calculated BDE in kJ/mol; TPs in the gray dashed box were identified in the headspace by GC−MS, whose formulae and structures need further validation; the other TPs were identified in the aqueous phase by LC-HRMS/MS, the most plausible structures of which are shown according to the confirmed formulae and MS^2 fragments).

carrier gas (i.e., helium) was 1 mL/min. The GC temperature was initially at 30 °C, held for 1 min, increased to 150 °C at 5 °C min^{-1}, then increased to 250 °C at 50 °C min^{-1}, and held for 4 min. The total run time was 31 min. EI was performed using electrons with a kinetic energy of 70 eV. Data acquisition was performed in a positive mode with a full scan (m/z 40−300). MS fragments of plausible TPs were interpreted based on the following criteria: (1) no detection in the matrix blank and (2) the same retention time for all fragments of one product.

GC-MSD Analysis for Chlorinated Solvents. Chlorinated ethenes and ethene in all experimental samples fed with TCE/*cis*-DCE were regularly measured by injecting 500 μL of the headspace sample into a GC-MSD system (6850 Network GC system, 5975C VL MSD) equipped with an Rtx-200 capillary column (30 m × 250 μm × 1 μm; Shimadzu, Columbia, MD). The oven temperature was programmed to hold at 45 °C for 1 min, increased to 200 °C in 3.44 min, and held at 200 °C for 1 min. The temperatures of the injector and the detector were maintained at 220 and 250 °C, respectively. Data acquisition was performed at the selected ion monitoring mode.

Bond Dissociation Energy Calculation. The GAUSSIAN 09 quantum chemistry package was used to obtain the C−F bond dissociation energies (BDEs) for the parent compound and TPs examined in Figure 2. All molecular structures were optimized at the B3LYP/6-311+G(2d,2p) level of theory.[40−43] Grimme's empirical dispersion correction with Becke−Johnson damping was employed to approximate the dispersion interaction between molecules.[44] The SMD continuum solvation model was selected to simulate the solvent effect implicitly.[45] Frequency examinations of all optimized geometries were done to confirm that the local minima were reached instead of obtaining the first-order saddle point. The BDE for each C−F bond was calculated through a previously reported formula

$$\mathrm{BDE} = (H^*_{\mathrm{radical[PFASminusF]}} + H^*_{\mathrm{radicalF}}) - H^*_{\mathrm{parentPFAS}}$$

where H^* represents the enthalpy of formation.[8]

DNA Extraction and Quantitative Polymerase Chain Reaction. Biomass from 0.5 mL of the culture was sampled from each biological replicate. Microbial genomic DNA was extracted using a DNeasy PowerSoil Kit (QIAGEN, Germantown, MD) according to the manufacturer's instructions. Cell growth was measured by quantitative polymerase chain reaction (qPCR) using primers targeting universal bacterial 16S rRNA genes and 16S rRNA genes of *Dehalococcoides* spp., *Dehalobacter* spp., and *Geobacter* spp. (Table S3). Genomic DNAs of *D. mccartyi* FL2 and *D. restrictus* were quantified by NanoDrop One (Thermo Fisher Scientific) and served as qPCR standards. The relative abundance of reductive dehalogenase genes was determined by qPCR using the primers listed in Table S3. PowerUp SYBR Green reagents (Thermo Fisher Scientific) were used for qPCR according to the manufacturer's instructions. Briefly, every 20 μL reaction mixture contained 2.5 μL of the gDNA sample or serially diluted standard, 10 μL of 2× PowerUp SYBR Green master mix solution, and 1.25 μL of 10 μM forward and reverse primers. The PCR procedure included an initial deactivation at 95 °C for 2 min, followed by 40 thermal cycles at 95 °C for 1 s and then at 60 °C for 30 s.

Reverse-Transcription qPCR. RNA was extracted using acid-phenol/chloroform/isoamyl alcohol (25:24:1) and precipitated in ethanol at −20 °C as previously described.[46] RNA was cleaned up using the RNeasy PowerClean Pro CleanUp Kit (QIAGEN) according to the manufacturer's instructions. Contaminating DNA in the RNA samples was removed using a Turbo DNase Kit (Thermo Fisher Scientific) following the manufacturer's instructions. qPCR was carried out to verify the removal of genomic DNA contamination from the purified RNA. The quality of RNA was examined by agarose gel electrophoresis.

A SuperScript III First-Strand Synthesis System (Thermo Fisher Scientific) was applied for complementary DNA (cDNA) synthesis according to the manufacturer's instructions. In general, the 10 μL cDNA synthesis mix containing 8 μL of the RNA sample, 1 μL of the primer (random

https://dx.doi.org/10.1021/acs.est.0c04483
Environ. Sci. Technol. 2020, 54, 14393−14402

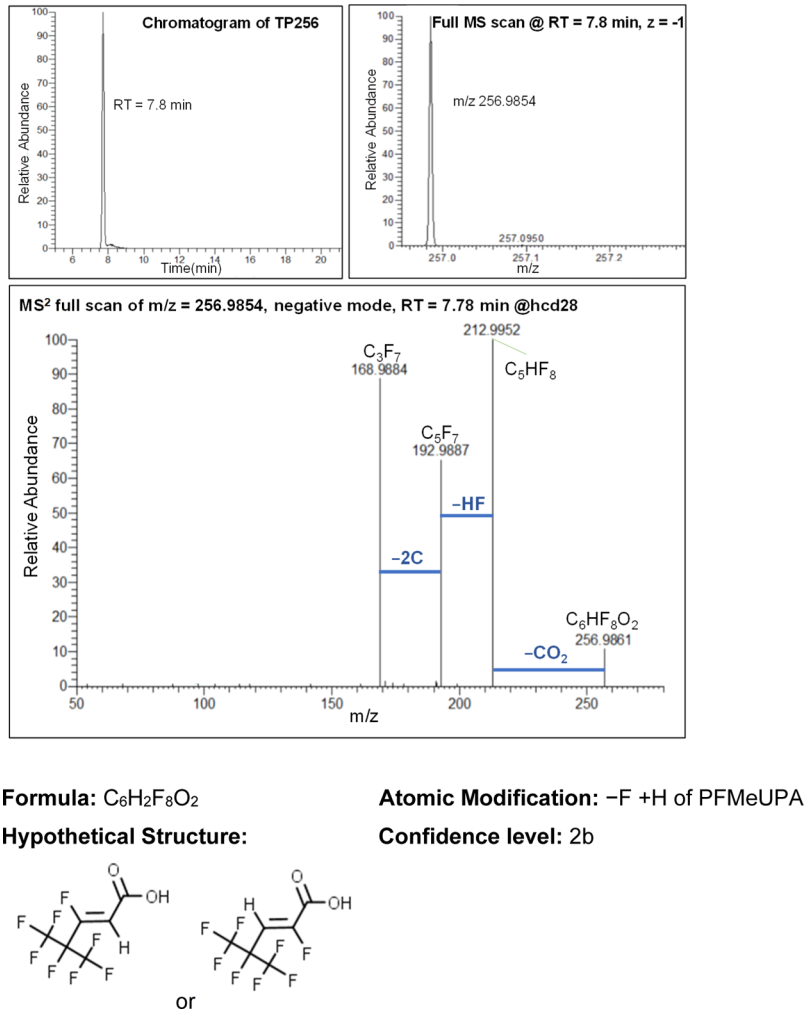

Figure 3. Structure elucidation of the first defluorination product of PFMeUPA (TP256).

hexamers), and 1 μL of 10 mM dNTP mix was incubated at 65 °C for 5 min and then placed on ice for 1 min. The cDNA synthesis mix was added to each RNA/primer mixture and incubated at 25 °C for 10 min and then at 50 °C for 50 min. The reaction was terminated at 85 °C for 5 min, and then, the entire tube was chilled on ice. At last, 1 μL of RNase H was added to each tube and incubated at 37 °C for 20 min. The cDNA synthesis products were stored at −20 °C for qPCR measurement using primers listed in Table S3.

The relative gene expression of RDase genes was calculated using the double-delta Ct method[47] (as shown in the following equation) with the *Dehalococcoides* 16S rRNA gene as the reference gene.

Relative gene expression = $2^{-\Delta\Delta Ct}$, where

$$\Delta\Delta Ct = \Delta Ct_{\text{Organofluorine-added sample}} - \Delta Ct_{\text{TCE-added control}}, \Delta Ct = Ct_{\text{RDase gene}} - Ct_{\text{16S rRNA gene}}$$

RESULTS AND DISCUSSION

Microbial Reductive Defluorination of a C_6 Perfluorinated Compound. The reductive defluorination was conducted in subsequent transfers (10%, v/v) of a well-studied and commercially available dechlorinating enrichment culture KB-1 (SiREM, Ontario, Canada). We investigated three perfluorinated compounds that exhibited abiotic reductive defluorination activities in a Ti(III)−vitamin B_{12} catalytic system[8] as well as two polyfluorinated compounds structurally similar to the C_6 perfluorinated compound (see compound details in the Materials and Methods section, Table S1). We obtained strong evidence for microbial reductive defluorination of the C_6 perfluorinated compound (i.e., PFMeUPA) as well as the polyfluorinated FTMeUPA in the following aspects: (i) complete parent compound biotransformation in biological samples but not in the heat-inactivated control (Figure 1A,B), indicating microbially/enzymatically mediated biotransformation; (ii) significant F^- release (Figure 1A,B) with the formation of the corresponding defluorination products (Figure 2A−D), indicating reductive defluorination; and (iii) no defluorination activity when no electron donor was provided, thus excluding defluorinating fermentation (Figure S4). For the saturated perfluorinated structures (PFOA and PFdiMeOA) or the saturated polyfluorinated structure (FTMePA), no microbial defluorination was observed (Figure S5), suggesting that the double bond (C═C) was crucial for the microbial reductive defluorination of FTMeUPA.

TP Analysis Reveals the C−F Bond Cleavage Positions and the Biotransformation Pathways of PFMeUPA and FTMeUPA. We have identified the major TPs for PFMeUPA and FTMeUPA according to the LC-

https://dx.doi.org/10.1021/acs.est.0c04483
Environ. Sci. Technol. 2020, 54, 14393−14402

HRMS/MS data (see details in the Materials and Methods section). Authentic standards were used to confirm the structures of some TPs in Figure 2C,D. For those without available authentic standards, the TP structures were inferred according to the MS^2 fragmentation patterns and the model-predicted MS^2 spectra[36] (Materials and Methods, Tables S1 and S2, Figures 3 and S6−S11). Because of the difference in MS ionization efficiency among different organofluorine structures (Table S4), the peak areas were only used to indicate the formation trend of individual TPs but not their relative abundance.

The TP profiles indicate two major biotransformation pathways: reductive defluorination and hydrogenation. The first-step, reductive defluorination, is the major reaction leading to the significant F^- release from PFMeUPA, forming TP256 (−F + H) (Figure 2A and Reaction 1 in Figure 2C). TP256 has an MS^2 fragment of $C_3F_7^-$, representing the intact branched tail in the structure (Figure 3). It indicates that the first C−F bond cleavage was at the sp^2 carbons of the double bond rather than at the sp^3 ones. It appears that the sp^2 C−F bonds are more readily for reductive defluorination, despite their higher BDE than the tertiary sp^3 C−F bond in PFMeUPA (Figure 2C). Similarly, the first C−F bond cleavage also occurred at the sp^2 carbon during the B_{12}-catalyzed abiotic reductive defluorination of another unsaturated compound 2,3,3,3-tetrafluoropropene.[2] The C═C bond provides a readily binding site for catalysts containing a transition metal, such as Co, Fe, Ni, and Mn, which can carry out reductive defluorination of unsaturated organofluorines in abiotic catalytic systems.[2,8,48−50]Similarly, the C═C bond may facilitate the binding of the defluorinating enzymes, which likely possess a metal center, to initiate the reductive defluorination. All the above-mentioned metals are also biologically relevant and could be the catalytic center of defluorinating enzymes, which may or may not be B_{12}-dependent. Investigating an extended list of unsaturated/saturated and branched/linear organofluorines and identifying and isolating the responsible defluorinating enzymes/microorganisms are needed in future studies to fully demonstrate the actual roles of the double bond (C═C) and B_{12} in the microbial reductive defluorination. In FTMeUPA, which is unsaturated but lacks sp^2 C−F bonds, the reductive defluorination occurred at one sp^3 C−F bond, most likely the tertiary sp^3 C−F bond that has a much lower BDE than the primary sp^3 C−F bonds, forming the corresponding TP221 (Figure 2B and Reaction 5 in Figure 2D).

Besides reductive defluorination, the other major pathway for both PFMeUPA and FTMeUPA was hydrogenation, forming the corresponding saturated carboxylic acids (TP276 and TP241; Reaction 2 in Figure 2C and Reaction 4 in Figure 2D, respectively). The hydrogenation pathway occurred in parallel with the reductive defluorination pathway because the hydrogenation products of PFMeUPA and FTMeUPA (i.e., TP276 and TP241) were accumulated to a plateau without a further decrease (Figure 2A,B). It appears that the saturated products were more recalcitrant to reductive defluorination than the unsaturated parent compounds, again suggesting the important role of the C═C bond. The hydrogenation of unsaturated polyfluorinated carboxylic acids is not uncommon and has been observed in both aerobic and anaerobic sludges.[19,21] The hydrogenation of α,β-unsaturated carboxylic anions forming the corresponding saturated carboxylic acids can be catalyzed by enoate reductases with nicotinamide−adenine−dinucleotide as the cofactor from anaerobic microorganisms such as *Clostridium kluyveri*.[51] In addition, flavin-based ene-reductases from the "Old Yellow Enzyme" family possessed by a variety of microorganisms may also carry out the reduction of activated alkenes that contain a carboxyl as the electron-withdrawing group (EWG) and an additional EWG such as a halogen.[52] However, it is still unclear whether microorganisms can obtain energy for growth from such hydrogenation reactions.

Microbial Preference between the Two Major Biotransformation Pathways of PFMeUPA and FTMeUPA. It is worth noting that although FTMeUPA was biotransformed faster than PFMeUPA (∼70 days vs ∼130 days for >90% removal), the F^- released from FTMeUPA was less and slower (Figure 1). The defluorination degree of the removed FTMeUPA during the entire incubation period was 4−5%, which is much lower than what would have been expected if all FTMeUPA was subject to the first-step reductive defluorination (i.e., one out of seven F, corresponding to 14%). In contrast, the defluorination degree of the removed PFMeUPA was about the same as that if all PFMeUPA underwent the first-step reductive defluorination (i.e., one out of nine F, corresponding to 11%). This result indicates that the reductive defluorination at the sp^2 C−F bond was favored over the hydrogenation pathway for PFMeUPA, whereas the sp^3 C−F bond cleavage was less favorable than the hydrogenation of the F-free sp^2 carbons for FTMeUPA. In addition, if the accumulation of TP276 (Figure 2A) was in a significant amount, the total 11% defluorination of PFMeUPA would suggest a secondary defluorination. However, we were not able to determine the accurate portions of PFMeUPA that underwent reductive defluorination and hydrogenation because of the lack of reference standards of TP256 and TP276. According to the LC-HRMS/MS results, we observed a further transformation of TP256 after 90 days (Figure 2A), but the only identified secondary TP (TP259) is a hydrogenation product of TP256 (Reaction 3 in Figure 2C). Plausible secondary defluorination TPs, including FTMeUPA and its TPs (i.e., TP221 and TP241), were not observed during the biotransformation of PFMeUPA. Thus, the secondary defluorination products of PFMeUPA, if any, could be smaller molecules that are not detectable by LC-HRMS/MS. We further used gas chromatography−mass spectrometry (GC−MS) to identify possible secondary defluorination products from the headspace. According to GC−MS fragment interpretation, we identified two plausible secondary defluorination products (Figure S12A,B). They were two olefin isomers with the second sp^2 C−F bond or the tertiary sp^3 C−F bond cleaved. As we did not detect the corresponding carboxylic acids of these two olefins by LC−MS/MS and the GC−MS data indicated the presence of the decarboxylation product of TP256 (Figure S12C), the second C−F bond cleavage likely occurred after the decarboxylation of TP256. Because of the low resolution of GC−MS and the lack of standards, the structures of the two secondary defluorination products could not be validated or quantified. The preferred position of the second C−F bond cleavage remains elusive. Collectively, the cleavage of the first C−F bond in a perfluorinated structure is more critical and of greater significance given the recalcitrance of perfluorinated structures to biodegradation. Our findings suggest that the presence of the C═C bond in a perfluorinated structure plays a crucial role in initiating the first C−F bond cleavage, which can result

https://dx.doi.org/10.1021/acs.est.0c04483
Environ. Sci. Technol. 2020, 54, 14393−14402

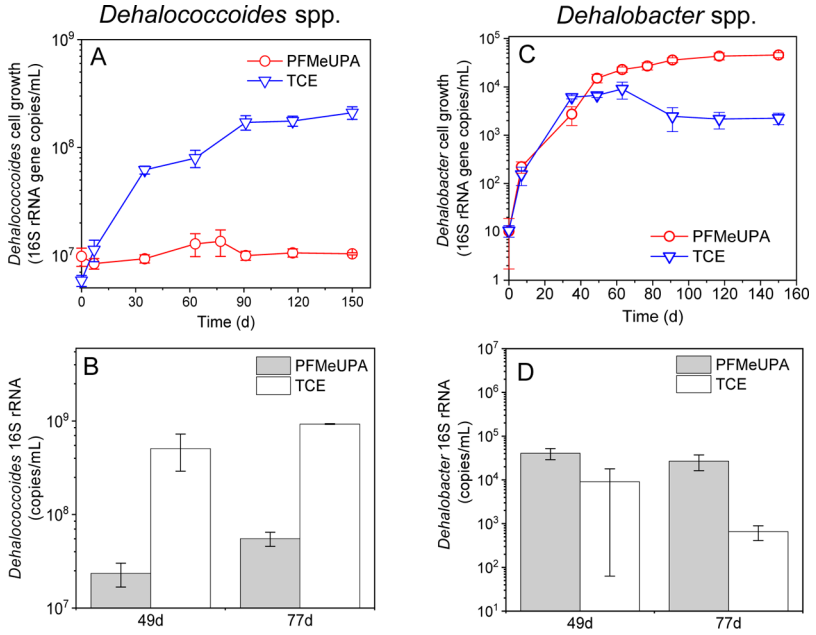

Figure 4. Growth (as 16S rRNA gene copy numbers) (A) and activities (as 16S rRNA copy numbers) (B) of *Dehalococcoides* spp. and the growth (C) and activities (D) of *Dehalobacter* spp. in KB-1 subcultures (10% v/v inoculation of KB-1) fed with ∼75 μM PFMeUPA compared to those grown on TCE (n = 3).

in the formation of polyfluorinated structures with C−H bond(s) that are more vulnerable to attack by other environmental microorganisms under aerobic or anaerobic conditions.[21,53,54]

Microbial Reductive Defluorination Capabilities of the Identified Dehalorespiring Microorganisms in the Community. The dominant dehalorespiring microorganism in the investigated KB-1 culture is *Dehalococcoides* spp..[55] The versatility of B_{12}-dependent reductive dehalogenases of *Dehalococcoides* spp. in metabolizing various organohalides makes them the most promising candidates capable of microbial reductive defluorination of the two fluorinated compounds.[56] Thus, we first looked at the growth and activities of *Dehalococcoides* spp. in the PFMeUPA/FTMeUPA-fed culture, in terms of the 16S rRNA gene abundance and its transcriptional levels, as well as the transcriptional levels of 14 RDase genes[57] identified in the community. Unexpectedly, no *Dehalococcoides* growth or RDase gene transcription was observed during the incubation period when PFMeUPA/FTMeUPA was provided as the sole electron acceptor (Figures 4A,B, S13, and S14). In comparison, cultures with TCE addition exhibited active growth of *Dehalococcoides* (Figures 4A,B and S13). Theoretically, the energy generated from the added PFMeUPA/FTMeUPA (∼75 μM) could sustain the growth of *Dehalococcoides* via reductive dehalogenation if it occurred. Therefore, the dominant chloroethene-respiring *Dehalococcoides* spp. in the community were not responsible for the reductive defluorination. It was corroborated by the two isolated *Dehalococcoides* strains, *D. mccartyi* FL2 and BAV1, not being able to cleave F^- from PFMeUPA but exhibiting reductive dechlorination activities (Figure S15).

We then looked at the growth of another two dechlorinators in this community: the second dominant TCE-dechlorinating species *Geobacter* spp.[55] and the minor dechlorinating species *Dehalobacter* spp..[58] Again, *Geobacter* spp. showed no growth in the PFMeUPA-fed culture and hence were not responsible for the reductive defluorination (Figure S16). Nevertheless, we observed significantly higher growth and activities of *Dehalobacter* in the PFMeUPA/FTMeUPA-fed culture compared to that in the TCE-fed ones (Figures 4C,D and S17). One should note that the initial abundance of *Dehalobacter* in the seed culture fed with TCE was extremely low (<10^3/mL). Such a low *Dehalobacter* abundance was consistent with what was observed in the TCE-fed subcultures of the same microbial community.[58] Several *Dehalobacter* strains have been demonstrated to biodegrade chlorinated compounds such as TCE, trichloroethane, and Trichlorobenzene (TCB).[58−60] A similar emergence of *Dehalobacter* population with a significant decrease of *Dehalococcoides* population was observed when the terminal electron acceptor was switched from TCE to 1,2,4-TCB.[58] The abilities of *Dehalobacter* spp. to utilize diverse chlorinated compounds to alleviate substrate competition with other dehalorespiring microorganisms make them likely involved in the defluorination of PFMeUPA and FTMeUPA. Thus, we further examined the defluorination capabilities of the pure culture of *D. restrictus* strain PER-K23, the closest strain to *Dehalobacter* spp. in the community.[58] *D. restrictus* strain PER-K23 is known as an obligate organohalide-respiring bacterium, which is able to dechlorinate tetrachloroethene or TCE with hydrogen as the sole electron donor.[61] However, we did not detect any F^- release from PFMeUPA and FTMeUPA (Figure S18). As *Dehalobacter* spp. in the community showed higher growth and activities when fed with PFMeUPA/FTMeUPA than TCE, one may still not exclude the possibility that the actual *Dehalobacter* spp. in the community had different physiological characteristics and were able to carry out the reductive defluorination of PFMeUPA/FTMeUPA. Alternatively, they could carry out the biotransformation of primary intermediates, such as the first C−F bond cleavage product TP256 of PFMeUPA, thus dependent on the microorganisms involved in the primary biotransformation. Microorganisms responsible for the reductive defluorination may also be other members in the community, which are quite different from those for reductive

https://dx.doi.org/10.1021/acs.est.0c04483
Environ. Sci. Technol. 2020, 54, 14393−14402

dechlorination, and the responsible enzymes were different from the known B_{12}-dependent RDases.

Environmental Relevance. According to this study, microbial reductive defluorination of $>C_2$ perfluorinated compounds does exist in nature. The unsaturated structures seem to be more bioavailable, and the first C−F bond cleavage at the sp^2 position is a crucial first step to destruct perfluorinated structures, which could lead to further defluorination of the formed polyfluorinated products by environmental microorganisms. As the dominant dechlorinating species in the community were not responsible for the reductive defluorination, the actual defluorinating microorganisms were likely those in low abundances. Thus, higher defluorinating activities and perhaps a wider fluorinated substrate range would be expected for enriched and/or isolated defluorinating microorganisms. Therefore, future studies are needed to enrich and/or isolate the microorganisms responsible for the reductive defluorination and characterize their physiological properties in the highly enriched cultures and/or isolates. While the enrichment, identification, and isolation are still ongoing because of the slow growth of the defluorinating microorganisms, unveiling the microbial pathways of breaking the "hardest-ever" carbon−halogen bond via reductive dehalogenation has already initiated one significant step further toward a complete understanding of anaerobic microbial reductive defluorination.

In recent years, some short-chain ($\leq C_6$), branched, and unsaturated organofluorine compounds have already been used as alternatives to the legacy perfluoroalkyl substances and PFASs (e.g., PFOA and PFOS), and some have been detected in various environments as the original forms and the transformed forms from certain parent PFASs.[62,63] Given the increasing concerns of PFASs worldwide, the findings here will provide important implications and open up diverse venues for both fundamental science and engineering applications. These include identifying and characterizing the defluorinating microorganisms/enzymes for potential bioremediation strategies as well as assessing the environmental fate and biodegradability of PFASs, particularly for the unsaturated and/or branched perfluorinated structures. In addition, as PFASs cannot be completely phased out in the short term,[64] the structural specificity of biodefluorination may provide implications to the molecular design of fluorochemicals with enhanced biodegradability, a shorter half-life, and hence less bioaccumulability.

■ ASSOCIATED CONTENT

Supporting Information

The Supporting Information is available free of charge at https://pubs.acs.org/doi/10.1021/acs.est.0c04483.

Standard compound information; transformation product information; primer set information; comparison of selected PFAS ionization efficiencies; TCE, *cis*-DCE, and VC in the culture with only TCE added; comparison of F^- measured by ISE and IC using mock samples and real supernatant samples with standard addition; representative IC chromatogram showing all peaks detected in the culture medium matrix during the full elution period; fluoride-ion release from PFMeUPA without the electron donor; fluoride-ion release from 100 μM of FTMePA, PFdiMeOA, and PFOA in the dechlorinating microbial community; MS^2 fragments of PFMeUPA; TP276 structure elucidation; and TP259 structure elucidation (PDF)

■ AUTHOR INFORMATION

Corresponding Author

Yujie Men − *Department of Chemical and Environmental Engineering, University of California, Riverside, California 92521, United States; Department of Civil and Environmental Engineering, University of Illinois at Urbana-Champaign, Urbana, Illinois 61801, United States;* orcid.org/0000-0001-9811-3828; Phone: (951) 827-2820; Email: ymen@engr.ucr.edu, menyjam@gmail.com

Authors

Yaochun Yu − *Department of Chemical and Environmental Engineering, University of California, Riverside, California 92521, United States; Department of Civil and Environmental Engineering, University of Illinois at Urbana-Champaign, Urbana, Illinois 61801, United States;* orcid.org/0000-0001-9231-6026

Kunyang Zhang − *Department of Civil and Environmental Engineering, University of Illinois at Urbana-Champaign, Urbana, Illinois 61801, United States*

Zhong Li − *Metabolomics Center, University of Illinois at Urbana-Champaign, Urbana, Illinois 61801, United States*

Changxu Ren − *Department of Chemical and Environmental Engineering, University of California, Riverside, California 92521, United States;* orcid.org/0000-0002-1109-794X

Jin Chen − *Environmental Toxicology Graduate Program, University of California, Riverside, California 92521, United States;* orcid.org/0000-0002-6034-9971

Ying-Hsuan Lin − *Environmental Toxicology Graduate Program and Department of Environmental Sciences, University of California, Riverside, California 92521, United States;* orcid.org/0000-0001-8904-1287

Jinyong Liu − *Department of Chemical and Environmental Engineering, University of California, Riverside, California 92521, United States;* orcid.org/0000-0003-1473-5377

Complete contact information is available at: https://pubs.acs.org/10.1021/acs.est.0c04483

Notes

The authors declare no competing financial interest.

■ ACKNOWLEDGMENTS

We would like to acknowledge Jennifer Webb, Sandra Dworatzek, and Jeff Roberts from SiREM for generously providing the KB-1 culture. This study was supported by the National Science Foundation (Award no. CHE-1709286 for K.Z., Y.Y., and Y.M. and CHE-1709719 for C.R. and J.L.) and the Strategic Environmental Research and Development Program (ER20-1541 for Y.Y. and Y.M.).

■ REFERENCES

(1) Wang, Z.; DeWitt, J. C.; Higgins, C. P.; Cousins, I. T. A never-ending story of per- and polyfluoroalkyl substances (PFASs)? *Environ. Sci. Technol.* **2017**, *51*, 2508−2518.

(2) Im, J.; Walshe-Langford, G. E.; Moon, J.-W.; Löffler, F. E. Environmental fate of the next generation refrigerant 2,3,3,3-tetrafluoropropene (HFO-1234yf). *Environ. Sci. Technol.* **2014**, *48*, 13181−13187.

(3) Furuya, T.; Kamlet, A. S.; Ritter, T. Catalysis for fluorination and trifluoromethylation. *Nature* **2011**, *473*, 470−477.

(4) Xiao, F. Emerging poly- and perfluoroalkyl substances in the aquatic environment: a review of current literature. *Water Res.* **2017**, *124*, 482−495.
(5) Sun, M.; Arevalo, E.; Strynar, M.; Lindstrom, A.; Richardson, M.; Kearns, B.; Pickett, A.; Smith, C.; Knappe, D. R. U. Legacy and emerging perfluoroalkyl substances are important drinking water contaminants in the Cape Fear River watershed of North Carolina. *Environ. Sci. Technol. Lett.* **2016**, *3*, 415−419.
(6) Lindstrom, A. B.; Strynar, M. J.; Delinsky, A. D.; Nakayama, S. F.; McMillan, L.; Libelo, E. L.; Neill, M.; Thomas, L. Application of WWTP biosolids and resulting perfluorinated compound contamination of surface and well water in Decatur, Alabama, USA. *Environ. Sci. Technol.* **2011**, *45*, 8015−8021.
(7) Key, B. D.; Howell, R. D.; Criddle, C. S. Fluorinated organics in the biosphere. *Environ. Sci. Technol.* **1997**, *31*, 2445−2454.
(8) Liu, J.; Van Hoomissen, D. J.; Liu, T.; Maizel, A.; Huo, X.; Fernández, S. R.; Ren, C.; Xiao, X.; Fang, Y.; Schaefer, C. E.; Higgins, C. P.; Vyas, S.; Strathmann, T. J. Reductive defluorination of branched per- and polyfluoroalkyl substances with cobalt complex catalysts. *Environ. Sci. Technol. Lett.* **2018**, *5*, 289−294.
(9) Bentel, M. J.; Yu, Y.; Xu, L.; Li, Z.; Wong, B. M.; Men, Y.; Liu, J. Defluorination of per- and polyfluoroalkyl substances (PFASs) with hydrated electrons: structural dependence and implications to PFAS remediation and management. *Environ. Sci. Technol.* **2019**, *53*, 3718−3728.
(10) Merino, N.; Qu, Y.; Deeb, R. A.; Hawley, E. L.; Hoffmann, M. R.; Mahendra, S. Degradation and removal methods for perfluoroalkyl and polyfluoroalkyl substances in water. *Environ. Eng. Sci.* **2016**, *33*, 615−649.
(11) Bentel, M. J.; Yu, Y.; Xu, L.; Kwon, H.; Li, Z.; Wong, B. M.; Men, Y.; Liu, J. Degradation of perfluoroalkyl ether carboxylic acids with hydrated electrons: structure-reactivity relationships and environmental implications. *Environ. Sci. Technol.* **2020**, *54*, 2489−2499.
(12) Bentel, M. J.; Liu, Z.; Yu, Y.; Gao, J.; Men, Y.; Liu, J. Enhanced degradation of perfluorocarboxylic acids (PFCAs) by UV/Sulfite treatment: reaction mechanisms and system efficiencies at pH 12. *Environ. Sci. Technol. Lett.* **2020**, *7*, 351−357.
(13) Goldman, P. The enzymatic cleavage of the carbon-fluorine bond in fluoroacetate. *J. Biol. Chem.* **1965**, *240*, 3434−3438.
(14) Visscher, P. T.; Culbertson, C. W.; Oremland, R. S. Degradation of trifluoroacetate in oxic and anoxic sediments. *Nature* **1994**, *369*, 729−731.
(15) Kim, B. R.; Suidan, M. T.; Wallington, T. J.; Du, X. Biodegradability of trifluoroacetic acid. *Environ. Eng. Sci.* **2000**, *17*, 337−342.
(16) Oremland, R. S.; Matheson, L. J.; Guidetti, J. R.; Schaefer, J. K.; Visscher, P. T. *Summary of research results on bacterial degradation of trifluoroacetate (TFA), November, 1994-May, 1995; Open-File Report*, 1995; Vol. *95*−*422*.
(17) Davis, C. K.; Webb, R. I.; Sly, L. I.; Denman, S. E.; McSweeney, C. S. Isolation and survey of novel fluoroacetate-degrading bacteria belonging to the phylum Synergistetes. *FEMS Microbiol. Ecol.* **2012**, *80*, 671−684.
(18) Leong, L. E. X.; Denman, S. E.; Hugenholtz, P.; McSweeney, C. S. Amino acid and peptide utilization profiles of the fluoroacetate-degrading bacterium Synergistetes strain MFA1 under varying conditions. *Microb. Ecol.* **2016**, *71*, 494−504.
(19) Wang, N.; Szostek, B.; Buck, R. C.; Folsom, P. W.; Sulecki, L. M.; Capka, V.; Berti, W. R.; Gannon, J. T. Fluorotelomer alcohol biodegradation-direct evidence that perfluorinated carbon chains breakdown. *Environ. Sci. Technol.* **2005**, *39*, 7516−7528.
(20) Shaw, D. M. J.; Munoz, G.; Bottos, E. M.; Duy, S. V.; Sauvé, S.; Liu, J.; Van Hamme, J. D. Degradation and defluorination of 6:2 fluorotelomer sulfonamidoalkyl betaine and 6:2 fluorotelomer sulfonate by Gordonia sp. strain NB4-1Y under sulfur-limiting conditions. *Sci. Total Environ.* **2019**, *647*, 690−698.
(21) Zhang, S.; Szostek, B.; McCausland, P. K.; Wolstenholme, B. W.; Lu, X.; Wang, N.; Buck, R. C. 6:2 and 8:2 fluorotelomer alcohol anaerobic biotransformation in digester sludge from a WWTP under methanogenic conditions. *Environ. Sci. Technol.* **2013**, *47*, 4227−4235.
(22) Liu, J.; Mejia Avendaño, S. Microbial degradation of polyfluoroalkyl chemicals in the environment: a review. *Environ. Int.* **2013**, *61*, 98−114.
(23) Huang, S.; Jaffé, P. R. Defluorination of perfluorooctanoic acid (PFOA) and perfluorooctane sulfonate (PFOS) by Acidimicrobium sp. strain A6. *Environ. Sci. Technol.* **2019**, *53*, 11410−11419.
(24) Parsons, J. R.; Sáez, M.; Dolfing, J.; de Voogt, P. Biodegradation of perfluorinated compounds. In *Reviews of Environmental Contamination and Toxicology*; Whitacre, D. M., Ed.; Springer US: New York, NY, 2008; Vol. *196*; pp 53−71.
(25) Park, S.; de Perre, C.; Lee, L. S. Alternate reductants with VB12 to transform C8 and C6 perfluoroalkyl sulfonates: limitations and insights into isomer specific transformation rates, products and pathways. *Environ. Sci. Technol.* **2017**, *51*, 13869−13877.
(26) Brown, K. L. Chemistry and enzymology of vitamin B_{12}. *Chem. Rev.* **2005**, *105*, 2075−2150.
(27) Fincker, M.; Spormann, A. M. Biochemistry of catabolic reductive dehalogenation. *Annu. Rev. Biochem.* **2017**, *86*, 357−386.
(28) Schubert, T.; Adrian, L.; Sawers, R. G.; Diekert, G. Organohalide respiratory chains: composition, topology and key enzymes. *FEMS Microbiol. Ecol.* **2018**, *94*, fiy035.
(29) Holliger, C.; Regeard, C.; Diekert, G. Dehalogenation by anaerobic bacteria. In *Dehalogenation*; Häggblom, M. M.; Bossert, I. D., Eds.; Springer: Boston, MA, 2004; pp 115−157.
(30) Men, Y.; Feil, H.; VerBerkmoes, N. C.; Shah, M. B.; Johnson, D. R.; Lee, P. K. H.; West, K. A.; Zinder, S. H.; Andersen, G. L.; Alvarez-Cohen, L. Sustainable syntrophic growth of Dehalococcoides ethenogenes strain 195 with Desulfovibrio vulgaris Hildenborough and Methanobacterium congolense: global transcriptomic and proteomic analyses. *ISME J.* **2012**, *6*, 410−421.
(31) He, J.; Holmes, V. F.; Lee, P. K. H.; Alvarez-Cohen, L. Influence of vitamin B12 and cocultures on the growth of Dehalococcoides isolates in defined medium. *Appl. Environ. Microbiol.* **2007**, *73*, 2847−2853.
(32) Han, P.; Yu, Y.; Zhou, L.; Tian, Z.; Li, Z.; Hou, L.; Liu, M.; Wu, Q.; Wagner, M.; Men, Y. Specific micropollutant biotransformation pattern by the comammox bacterium Nitrospira inopinata. *Environ. Sci. Technol.* **2019**, *53*, 8695−8705.
(33) Zhou, L.-J.; Han, P.; Yu, Y.; Wang, B.; Men, Y.; Wagner, M.; Wu, Q. L. Cometabolic biotransformation and microbial-mediated abiotic transformation of sulfonamides by three ammonia oxidizers. *Water Res.* **2019**, *159*, 444−453.
(34) Yu, Y.; Han, P.; Zhou, L.-J.; Li, Z.; Wagner, M.; Men, Y. Ammonia monooxygenase-mediated cometabolic biotransformation and hydroxylamine-mediated abiotic transformation of micropollutants in an AOB/NOB coculture. *Environ. Sci. Technol.* **2018**, *52*, 9196−9205.
(35) Men, Y.; Han, P.; Helbling, D. E.; Jehmlich, N.; Herbold, C.; Gulde, R.; Onnis-Hayden, A.; Gu, A. Z.; Johnson, D. R.; Wagner, M.; Fenner, K. Biotransformation of two pharmaceuticals by the ammonia-oxidizing archaeon Nitrososphaera gargensis. *Environ. Sci. Technol.* **2016**, *50*, 4682−4692.
(36) Allen, F.; Pon, A.; Wilson, M.; Greiner, R.; Wishart, D. CFM-ID: a web server for annotation, spectrum prediction and metabolite identification from tandem mass spectra. *Nucleic Acids Res.* **2014**, *42*, W94−W99.
(37) Schymanski, E. L.; Jeon, J.; Gulde, R.; Fenner, K.; Ruff, M.; Singer, H. P.; Hollender, J. Identifying small molecules via high resolution mass spectrometry: communicating confidence. *Environ. Sci. Technol.* **2014**, *48*, 2097−2098.
(38) Miller, M. E.; Stuart, J. D. Comparison of gas-sampled and SPME-sampled static headspace for the determination of volatile flavor components. *Anal. Chem.* **1999**, *71*, 23−27.
(39) Bourdin, D.; Desauziers, V. Development of SPME on-fiber derivatization for the sampling of formaldehyde and other carbonyl compounds in indoor air. *Anal. Bioanal. Chem.* **2014**, *406*, 317−328.

https://dx.doi.org/10.1021/acs.est.0c04483
Environ. Sci. Technol. 2020, 54, 14393−14402

(40) Becke, A. D. Density-functional thermochemistry. III. The role of exact exchange. *J. Chem. Phys.* **1993**, *98*, 5648−5652.
(41) Lee, C.; Yang, W.; Parr, R. G. Development of the Colle-Salvetti correlation-energy formula into a functional of the electron density. *Phys. Rev. B: Condens. Matter Mater. Phys.* **1988**, *37*, 785−789.
(42) Stephens, P. J.; Devlin, F. J.; Chabalowski, C. F.; Frisch, M. J. Ab initio calculation of vibrational absorption and circular dichroism spectra using density functional force fields. *J. Phys. Chem.* **1994**, *98*, 11623−11627.
(43) Vosko, S. H.; Wilk, L.; Nusair, M. Accurate spin-dependent electron liquid correlation energies for local spin density calculations: a critical analysis. *Can. J. Phys.* **1980**, *58*, 1200−1211.
(44) Grimme, S.; Ehrlich, S.; Goerigk, L. Effect of the damping function in dispersion corrected density functional theory. *J. Comput. Chem.* **2011**, *32*, 1456−1465.
(45) Marenich, A. V.; Cramer, C. J.; Truhlar, D. G. Universal solvation model based on solute electron density and on a continuum model of the solvent defined by the bulk dielectric constant and atomic surface tensions. *J. Phys. Chem. B* **2009**, *113*, 6378−6396.
(46) Men, Y.; Seth, E. C.; Yi, S.; Allen, R. H.; Taga, M. E.; Alvarez-Cohen, L. Sustainable growth of Dehalococcoides mccartyi 195 by corrinoid salvaging and remodeling in defined lactate-fermenting consortia. *Appl. Environ. Microbiol.* **2014**, *80*, 2133−2141.
(47) Livak, K. J.; Schmittgen, T. D. Analysis of relative gene expression data using real-time quantitative PCR and the $2^{-\Delta\Delta CT}$ method. *Methods* **2001**, *25*, 402−408.
(48) Baumgartner, R.; McNeill, K. Hydrodefluorination and hydrogenation of fluorobenzene under mild aqueous conditions. *Environ. Sci. Technol.* **2012**, *46*, 10199−10205.
(49) Peterson, A. A.; McNeill, K. Catalytic dehalogenation of sp^2 C-F and C-Cl bonds in fluoro- and chloroalkenes. *Organometallics* **2006**, *25*, 4938−4940.
(50) Amii, H.; Uneyama, K. C-F bond activation in organic synthesis. *Chem. Rev.* **2009**, *109*, 2119−2183.
(51) Tischer, W.; Bader, J.; Simon, H. Purification and some properties of a hitherto-unknown enzyme reducing the carbon-carbon double bond of α,β-unsaturated carboxylate anions. *Eur. J. Biochem.* **1979**, *97*, 103−112.
(52) Winkler, C. K.; Tasnádi, G.; Clay, D.; Hall, M.; Faber, K. Asymmetric bioreduction of activated alkenes to industrially relevant optically active compounds. *J. Biotechnol.* **2012**, *162*, 381−389.
(53) Li, F.; Su, Q.; Zhou, Z.; Liao, X.; Zou, J.; Yuan, B.; Sun, W. Anaerobic biodegradation of 8:2 fluorotelomer alcohol in anaerobic activated sludge: metabolic products and pathways. *Chemosphere* **2018**, *200*, 124−132.
(54) Wang, N.; Buck, R. C.; Szostek, B.; Sulecki, L. M.; Wolstenholme, B. W. 5:3 Polyfluorinated acid aerobic biotransformation in activated sludge via novel "one-carbon removal pathways". *Chemosphere* **2012**, *87*, 527−534.
(55) Duhamel, M.; Edwards, E. A. Microbial composition of chlorinated ethene-degrading cultures dominated by Dehalococcoides. *FEMS Microbiol. Ecol.* **2006**, *58*, 538−549.
(56) Löffler, F. E.; Yan, J.; Ritalahti, K. M.; Adrian, L.; Edwards, E. A.; Konstantinidis, K. T.; Müller, J. A.; Fullerton, H.; Zinder, S. H.; Spormann, A. M. Dehalococcoides mccartyi gen. nov., sp. nov., obligately organohalide-respiring anaerobic bacteria relevant to halogen cycling and bioremediation, belong to a novel bacterial class, Dehalococcoidia classis nov., order Dehalococcoidales ord. nov. and family Dehalococcoidaceae fam. nov., within the phylum Chloroflexi. *Int. J. Syst. Evol. Microbiol.* **2015**, *63*, 625−635.
(57) Waller, A. S.; Krajmalnik-Brown, R.; Löffler, F. E.; Edwards, E. A. Multiple reductive-dehalogenase-homologous genes are simultaneously transcribed during dechlorination by Dehalococcoides-containing cultures. *Appl. Environ. Microbiol.* **2005**, *71*, 8257−8264.
(58) Puentes Jácome, L. A.; Edwards, E. A. A switch of chlorinated substrate causes emergence of a previously undetected native Dehalobacter population in an established Dehalococcoides-dominated chloroethene-dechlorinating enrichment culture. *FEMS Microbiol. Ecol.* **2017**, *93*, fix141.
(59) Nelson, J. L.; Jiang, J.; Zinder, S. H. Dehalogenation of chlorobenzenes, dichlorotoluenes, and tetrachloroethene by three Dehalobacter spp. *Environ. Sci. Technol.* **2014**, *48*, 3776−3782.
(60) Alfán-Guzmán, R.; Ertan, H.; Manefield, M.; Lee, M. Isolation and characterization of Dehalobacter sp. strain TeCB1 including identification of TcbA: a novel tetra- and trichlorobenzene reductive dehalogenase. *Front. Microbiol.* **2017**, *8*, 558.
(61) Rupakula, A.; Kruse, T.; Boeren, S.; Holliger, C.; Smidt, H.; Maillard, J. The restricted metabolism of the obligate organohalide respiring bacterium Dehalobacter restrictus: lessons from tiered functional genomics. *Philos. Trans. R. Soc., B* **2013**, *368*, 20120325.
(62) Washington, J. W.; Jenkins, T. M.; Weber, E. J. Identification of unsaturated and 2H polyfluorocarboxylate homologous series and their detection in environmental samples and as polymer degradation products. *Environ. Sci. Technol.* **2015**, *49*, 13256−13263.
(63) Bao, Y.; Qu, Y.; Huang, J.; Cagnetta, G.; Yu, G.; Weber, R. First assessment on degradability of sodium p-perfluorous nonenoxybenzene sulfonate (OBS), a high volume alternative to perfluorooctane sulfonate in fire-fighting foams and oil production agents in China. *RSC Adv.* **2017**, *7*, 46948−46957.
(64) Cousins, I. T.; Goldenman, G.; Herzke, D.; Lohmann, R.; Miller, M.; Ng, C. A.; Patton, S.; Scheringer, M.; Trier, X.; Vierke, L.; Wang, Z.; DeWitt, J. C. The concept of essential use for determining when uses of PFASs can be phased out. *Environ. Sci.: Processes Impacts* **2019**, *21*, 1803−1815.

NOTE ADDED AFTER ASAP PUBLICATION

Originally published ASAP on October 29, 2020; Figure 2 revised on November 3, 2020.

https://dx.doi.org/10.1021/acs.est.0c04483
Environ. Sci. Technol. 2020, 54, 14393−14402